

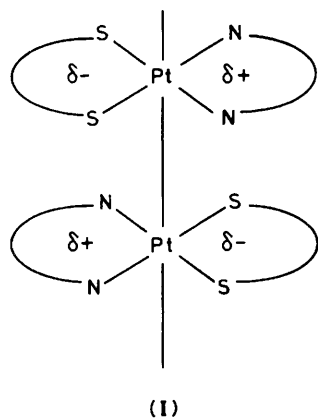
X-Ray Crystal Structure of (2,2'-Bipyrimidine)[1,2-dicyanoethylene-1,2-dithiolato(2-)]platinum(II)-*N,N*-Dimethylformamide and Properties of PtS₂N₂-type Complexes †

Gen-etsu Matsubayashi,* Yasuhiro Yamaguchi, and Toshio Tanaka

Department of Applied Chemistry, Faculty of Engineering, Osaka University, Yamadaoka, Suita, Osaka 565, Japan

PtS₂N₂-type complexes containing both an electron-donor dithiolate ligand, 1,2-dicyanoethylene-1,2-dithiolate(2-) (maleonitriledithiolate, mnt) or 4,5-dimercapto-1,3-dithiole-2-thionate(2-) (dmit), and a π-electron acceptor nitrogen ligand, 2,2'-bipyrimidine (bipym) or *N*-ethyl-2-methylpyridine-2-carbaldimine (epa), were isolated. The complexes are polarized in their ground states, exhibiting intense electronic absorption bands due to ligand-to-ligand charge-transfer transitions at 490–580 nm. On doping iodine into the dmit complexes they were partially oxidized to afford [Pt(dmit)L]_x (L = bipym or epa; x = 1.6–3.4) containing I₃⁻ or I₅⁻ ions, which behave as semiconductors with electrical conductivities of 1 × 10⁻⁴–1 × 10⁻⁷ S cm⁻¹ at 25 °C as compacted pellets. A single-crystal X-ray analysis of [Pt(mnt)(bipym)]·dmf (dmf = *N,N*-dimethylformamide) revealed a one-dimensional columnar packing of [Pt(mnt)(bipym)] molecules. The crystals are triclinic, space group *P*1̄, with cell dimensions *a* = 9.811(1), *b* = 12.792(1), *c* = 7.5367(9) Å, α = 100.73(1), β = 93.37(1), γ = 91.03(1)°, and *Z* = 2. Least-squares refinement, based on 3765 independent reflections with |*F*_o| > 3σ(*F*), converged at *R* = 0.062. Electronic states and molecular interactions of the PtS₂N₂-type complexes and their iodine-doped analogues are discussed on the basis of electronic, e.s.r., and X-ray photoelectron spectra.

Partially oxidized planar metal complexes often exhibit high electrical conductivities by forming one-dimensional molecular columns through metal–metal interactions.¹ Planar metal complexes with a polarized field in their ligands are expected to form columnar structures through metal–metal and interligand electrostatic interactions, which are suitable for an electrical conduction. Square-planar metal complexes containing both an electron-donor dithiolate ligand and a π-electron-acceptor pyridyl chelate ligand were reported to be polarized, showing



an intramolecular ligand-to-ligand charge-transfer absorption band.^{2–5} Platinum(II) complexes with both a planar dithiolate ligand and an N₂ chelate ligand containing a pyridyl or related ring may assume a columnar molecular packing (I) through

an S...N electrostatic interaction as well as a Pt...Pt contact and form effective electrical conduction pathways, if partially oxidized.

This paper reports preparations and properties of platinum(II) complexes both with a 1,2-dicyanoethylene-1,2-dithiolate(2-) (maleonitriledithiolate, mnt) or 4,5-dimercapto-1,3-dithiole-2-thionate(2-) (dmit) ligand as an electron donor and with 2,2'-bipyrimidine (bipym) or *N*-ethyl-2-methylpyridine-2-carbaldimine (epa) as a π-electron acceptor and electrical properties of their halogen-doped complexes. Molecular interactions of these complexes are discussed on the basis of electronic, e.s.r., and X-ray photoelectron spectra. The X-ray crystal structure of [Pt(mnt)(bipym)]·dmf (dmf = *N,N*-dimethylformamide) is also described.

Experimental

Materials.—Disodium 1,2-dicyanoethylene-1,2-dithiolate, Na₂(mnt),⁶ (2,2'-bipyrimidine)dichloroplatinum(II), [PtCl₂(bipym)],⁷ and dichloro(*N*-ethyl-2-methylpyridine-2-carbaldimine)platinum(II), [PtCl₂(epa)],⁷ were prepared according to the literature. 2,2'-Bipyrimidine was commercially available.

Preparation of PtS₂N₂-type Complexes.—A dimethyl sulphoxide (dmsO) (45 cm³) solution of [PtCl₂(bipym)] (270 mg, 640 μmol) was added to a methanol (10 cm³) solution of Na₂(mnt) (150 mg, 800 μmol) and the solution stirred for 10 h at room temperature. After concentration to half the volume, water (10 cm³) was added to afford a dark red precipitate, which was recrystallised from methanol–*N,N*-dimethylformamide (dmf) (1:1 v/v) to yield red crystals of [Pt(mnt)(bipym)]·dmf (1) (55% yield).

A methanol–dmf (5:1 v/v) (90 cm³) solution of Na₂(mnt) (340 mg, 1.8 mmol) was added to a methanol (20 cm³) solution of [PtCl₂(epa)] (640 mg, 1.6 mmol) and the solution allowed to stand in a refrigerator overnight to afford dark red microcrystals of [Pt(mnt)(epa)] (2) (60% yield).

† Supplementary data available: see Instructions for Authors, *J. Chem. Soc., Dalton Trans.*, 1988, Issue 1, pp. xvii–xx.

Non-S.I. unit employed: eV ≈ 1.60 × 10⁻¹⁹ J.

[Pt(dmit)(bipym)] (3) was prepared by reacting [PtCl₂-(bipym)] with Na₂(dmit) in methanol-dmsO (1:1 v/v) (90% yield), as described for [Pt(dmit)(bipy)] (bipy = 2,2'-bipyridine).⁵

[Pt(dmit)(epa)] (4) was prepared according to the literature method.⁵

Halogen-doping of the PtS₂N₂-type Complexes.—Finely powdered complex (3) (30 mg, 55 μmol) was suspended in a hexane (60 cm³) solution of iodine (76 mg, 170 μmol), and the suspension stirred for 22 h at room temperature under a nitrogen atmosphere. The resulting solid, [Pt(dmit)(bipym)]I_{1.6} (5), was washed with hexane, collected by filtration, and dried *in vacuo*. By a similar procedure, [Pt(dmit)(bipym)]I_{2.7} (6) was obtained by suspending (3) in hexane with 6 molar amounts of iodine. Complex (4) was also doped in a hexane suspension with 3 and 6 molar amounts of iodine to afford [Pt(dmit)(epa)]I_{1.9} (7) and [Pt(dmit)(epa)]I_{3.4} (8), respectively. On the other hand, (1) and (2) were not doped with iodine on suspension in hexane with excess amounts of iodine.

Bromine-doping was performed for (2), (3), and (4) suspended in hexane using 2 molar amounts of bromine to afford [Pt(mnt)(epa)]Br_{0.52} (9), [Pt(dmit)(bipym)]Br_{1.8} (10), and [Pt(dmit)(epa)]Br_{3.1} (11), respectively.

To a dmf (20 cm³) solution of (2) (140 mg, 0.28 mmol) was added bromine (180 mg, 1.1 mmol). The solution immediately turned dark blue. To the solution was added water (20 cm³) affording a greenish blue precipitate of [PtBr₂(mnt)(epa)] (12), which was collected by centrifugation, washed with water and methanol, and dried *in vacuo* (70% yield).

Elemental analyses for the complexes are listed in Table 1.

Physical Measurements.—Electronic absorption,⁸ powder reflectance,⁸ e.s.r.,⁹ X-ray photoelectron (x.p.s.),⁹ and Raman spectra¹⁰ were measured as described elsewhere. Electrical resistivities for compacted pellets of the complexes were measured by the conventional two-probe technique.¹¹ Cyclic voltammograms of the complexes were recorded in dmf as described previously.¹⁰

X-Ray Crystal Structure Analysis of [Pt(mnt)(bipym)]-dmf (1).—Oscillation and Weissenberg photographs indicated a triclinic system and the space group *P* $\bar{1}$ was found to be correct on the basis of the successful analysis. Accurate cell constants were determined by least-squares treatment of the angular coordinates of 25 independent reflections with 2θ in the range 22–33°, measured on a Rigaku four-circle automated diffractometer with Mo-K_α (λ = 0.710 69 Å) radiation at the Crystallographic Research Centre, Institute for Protein Research, Osaka University.

Crystal data. C₁₅H₁₃N₇OPtS₂, *M* = 566.5, triclinic, space group *P* $\bar{1}$, *a* = 9.811(1), *b* = 12.792(1), *c* = 7.5367(9) Å, α = 100.73(1), β = 93.37(1), γ = 91.03(1)°, *U* = 927.3(2) Å³, *Z* = 2, *D*_c = 2.029(1) g cm⁻³, *F*(000) = 540, μ(Mo-K_α) = 82.5 cm⁻¹.

A single crystal with dimensions 0.47 × 0.17 × 0.10 mm sealed in a glass tube was used for the data collection. Intensity data were collected by the above-mentioned diffractometer using graphite-monochromatized Mo-K_α radiation and the ω–2θ scan technique at a scan rate of 8° min⁻¹ in 2θ. The scan width in 2θ was (1.0 + 0.35tanθ)°. No significant intensity variation was observed throughout the data collection. The intensities were corrected for Lorentz and polarization effects as well as for absorption. A total of 4 263 independent intensities in the range 3 < 2θ < 55° were measured, of which 3 765 reflections with |*F*_o| > 3σ(*F*) were used for solving and refining the structure.

The structure was solved by the conventional heavy-atom

Table 1. Colours and elemental analyses of PtS₂N₂-type complexes and their halogen-doped derivatives

Complex	Colour	Analysis* (%)		
		C	H	N
(1) [Pt(mnt)(bipym)]-dmf	Red	31.7 (31.8)	2.35 (2.3)	17.0 (17.3)
(2) [Pt(mnt)(epa)]	Dark red	30.7 (30.7)	2.2 (2.15)	11.9 (11.9)
(3) [Pt(dmit)(bipym)]	Dark green	24.15 (24.05)	1.25 (1.1)	10.0 (10.2)
(4) [Pt(dmit)(epa)]	Black	25.0 (25.15)	2.15 (1.9)	4.8 (5.3)
(5) [Pt(dmit)(bipym)]I _{1.6}	Black	17.7 (17.55)	1.05 (0.8)	7.0 (7.45)
(6) [Pt(dmit)(bipym)]I _{2.7}	Black	15.0 (14.8)	0.8 (0.7)	5.95 (6.30)
(7) [Pt(dmit)(epa)]I _{1.9}	Black	17.35 (17.25)	1.35 (1.35)	3.4 (3.65)
(8) [Pt(dmit)(epa)]I _{3.4}	Black	14.0 (13.9)	1.15 (1.05)	2.8 (2.95)
(9) [Pt(mnt)(epa)]Br _{0.52}	Dark red	28.35 (28.2)	2.0 (1.95)	10.8 (10.95)
(10) [Pt(dmit)(bipym)]Br _{1.8}	Black	18.5 (19.05)	1.1 (0.9)	8.8 (8.1)
(11) [Pt(dmit)(epa)]Br _{3.1}	Black	17.2 (17.1)	1.45 (1.3)	3.4 (3.6)
(12) [PtBr ₂ (mnt)(epa)]	Blue-green	22.95 (22.9)	1.85 (1.6)	8.65 (8.9)

* Calculated values in parentheses.

Table 2. Atomic co-ordinates (× 10⁴; × 10³ for H) for [Pt(mnt)(bipym)]-dmf (1) with estimated standard deviations in parentheses

Atom	<i>x</i>	<i>y</i>	<i>z</i>
Pt	767.0(3)	-45.3(3)	2 251.6(5)
S(1)	2 929(2)	-313(2)	1 452(4)
S(2)	537(3)	-1 766(2)	2 468(4)
N(1)	5 351(11)	-2 465(10)	141(20)
N(2)	2 321(17)	-4 289(10)	1 707(26)
N(3)	-1 201(8)	331(7)	2 932(11)
N(4)	-2 720(9)	1 791(8)	3 260(14)
N(5)	-583(11)	3 064(6)	2 511(18)
N(6)	798(8)	1 532(7)	2 156(11)
C(1)	3 103(10)	-1 670(8)	1 363(14)
C(2)	2 097(11)	-2 281(8)	1 800(17)
C(3)	4 331(12)	-2 118(9)	671(19)
C(4)	2 229(13)	-3 403(9)	1 755(21)
C(5)	-1 496(10)	1 380(8)	2 914(14)
C(6)	-2 163(12)	-310(9)	3 276(15)
C(7)	-3 440(11)	61(10)	3 487(19)
C(8)	-3 704(11)	1 106(11)	3 584(19)
C(9)	-372(11)	2 037(8)	2 531(16)
C(10)	474(14)	3 626(10)	2 103(24)
C(11)	1 711(12)	3 183(9)	1 700(20)
C(12)	1 869(10)	2 112(9)	1 768(17)
H(6)	-232(14)	-123(10)	308(17)
H(7)	-407(19)	-34(15)	426(25)
H(8)	-458(13)	144(10)	362(17)
H(10)	46(19)	430(13)	191(23)
H(11)	239(18)	357(13)	164(22)
H(12)	282(16)	182(11)	137(20)
dmf molecule			
O	6 466(13)	7 637(8)	4 679(17)
N(7)	6 623(14)	5 907(10)	3 431(21)
C(13)	5 972(17)	6 768(12)	4 153(24)
C(14)	8 115(23)	5 984(18)	3 136(38)
C(15)	5 959(31)	4 862(17)	2 697(42)
H(13)	474(18)	670(13)	451(22)

Table 3. Selected bond lengths (Å) and angles (°) for [Pt(mnt)(bipym)]·dmf (1) with estimated standard deviations in parentheses

Pt-S(1)	2.254(2)	Pt-S(2)	2.245(3)
Pt-N(3)	2.069(8)	Pt-N(6)	2.033(9)
S(1)-C(1)	1.736(10)	S(2)-C(2)	1.742(11)
N(1)-C(3)	1.164(17)	N(2)-C(4)	1.132(18)
N(3)-C(5)	1.380(14)	N(3)-C(6)	1.307(15)
N(4)-C(5)	1.340(13)	N(4)-C(8)	1.355(16)
N(5)-C(9)	1.336(15)	N(5)-C(10)	1.334(18)
N(6)-C(9)	1.346(13)	N(6)-C(12)	1.352(14)
C(1)-C(2)	1.342(15)	C(1)-C(3)	1.428(16)
C(2)-C(4)	1.438(16)	C(5)-C(9)	1.450(15)
C(6)-C(7)	1.356(16)	C(7)-C(8)	1.356(19)
C(10)-C(11)	1.375(18)	C(11)-C(12)	1.392(17)
S(1)-Pt-S(2)	90.1(1)	S(1)-Pt-N(6)	95.3(2)
S(2)-Pt-N(3)	94.9(3)	N(3)-Pt-N(6)	79.7(3)
Pt-S(1)-C(1)	103.0(4)	Pt-S(2)-C(2)	102.9(4)
Pt-N(3)-C(5)	113.3(6)	Pt-N(3)-C(6)	127.7(7)
Pt-N(6)-C(9)	115.7(7)	Pt-N(6)-C(12)	126.6(7)
S(1)-C(1)-C(2)	121.8(8)	S(1)-C(1)-C(3)	116.6(8)
C(2)-C(1)-C(3)	121.5(10)	S(2)-C(2)-C(1)	122.1(8)
S(2)-C(2)-C(4)	115.3(9)	C(1)-C(2)-C(4)	122.5(10)
N(1)-C(3)-C(1)	178.3(12)	N(2)-C(4)-C(2)	179.3(15)
N(3)-C(4)-N(4)	123.5(10)	N(3)-C(5)-C(9)	115.5(9)
N(3)-C(6)-C(7)	118.8(11)	N(4)-C(5)-C(9)	121.0(10)
N(4)-C(8)-C(7)	120.3(10)	N(5)-C(9)-N(6)	125.6(10)
N(5)-C(9)-C(5)	118.7(10)	N(5)-C(10)-C(11)	122.6(22)
N(6)-C(9)-C(5)	115.7(7)	N(6)-C(12)-C(11)	119.5(10)
C(5)-N(3)-C(6)	119.0(9)	C(5)-N(4)-C(8)	116.2(10)
C(6)-C(7)-C(8)	121.6(11)	C(9)-N(5)-C(10)	116.2(10)
C(9)-N(6)-C(12)	117.7(9)	C(10)-C(11)-C(12)	118.3(11)

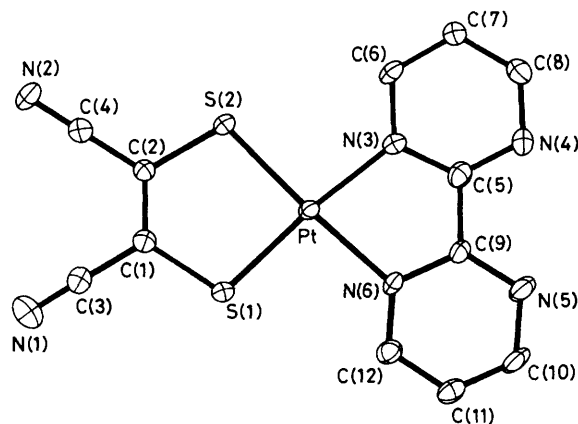
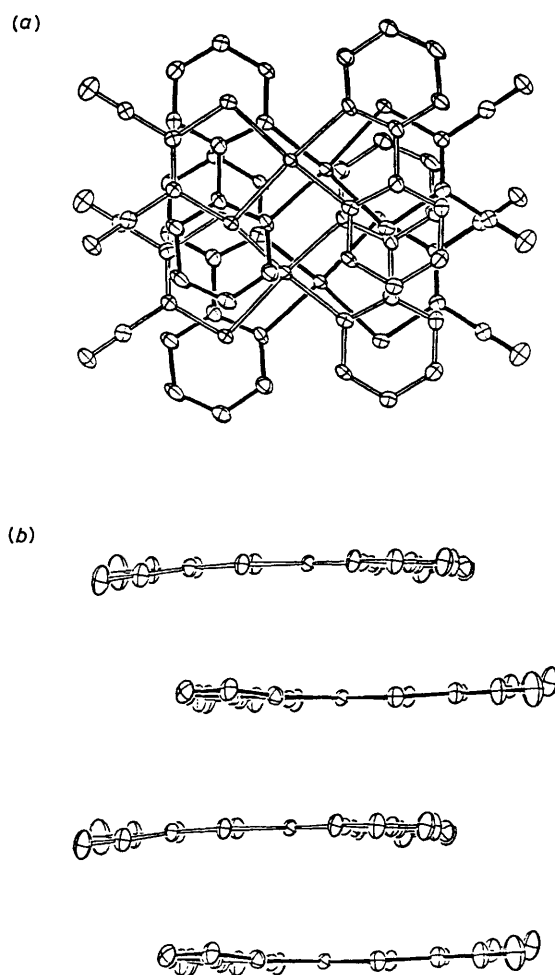
technique. Subsequent cycles of Fourier syntheses and block-diagonal least-squares calculations gave a reasonable set of co-ordinates for all the non-hydrogen atoms. A difference-Fourier map gave positions of all the hydrogen atoms of 2,2'-bipyrimidine and the aldehyde-hydrogen of the solvated dmf molecule. The final refinement with anisotropic thermal parameters for the non-hydrogen atoms and isotropic ones for hydrogen atoms converged at $R = \Sigma ||F_o| - |F_c|| / \Sigma |F_o| = 0.062$ and $R' = [\Sigma w(|F_o| - |F_c|)^2 / \Sigma w|F_o|^2]^{1/2} = 0.077$, using the weighting scheme $w^{-1} = \sigma^2(F_o) + 0.005F_o^2$. Atomic scattering factors were taken from ref. 12. The final atomic co-ordinates with estimated standard deviations are listed in Table 2.

Crystallographic calculations were performed on an ACOS 900S computer at the Crystallographic Research Centre, Osaka University. Figures for the crystal structures were drawn by the local version of the ORTEP-II program.¹³

Additional material available from the Cambridge Crystallographic Data Centre comprises thermal parameters and remaining bond lengths and angles.

Results and Discussion

Crystal Structure of [Pt(mnt)(bipym)]·dmf (1).—Figure 1 illustrates the molecular structure of complex (1). Relevant bond distances and angles are summarized in Table 3. The platinum atom is co-ordinated by two nitrogen and two sulphur atoms to form a square-planar geometry. The geometry about the platinum atom is almost planar (± 0.211 Å) except for the nitrile groups. The Pt-S distances [2.245(3) and 2.254(2) Å] are slightly shorter than those of other [Pt(mnt)₂]ⁿ⁻ complexes: Li_{0.75}[Pt(mnt)₂]·2H₂O (2.271 Å),¹⁴ Rb[Pt(mnt)₂]·2H₂O (av. 2.260 Å),¹⁵ Li_{0.5}[Pt(mnt)₂]·2H₂O (2.266 Å),¹⁶ and [H₃O]_{0.33}Li_{0.8}[Pt(mnt)₂]·1.67H₂O [2.271(2) Å].¹⁷ Other platinum complexes having a *trans* S-Pt-S linkage were reported to contain longer Pt-S distances: [Pt₂(S₂CC₆H₄Prⁱ)₄]

**Figure 1.** Molecular structure of [Pt(mnt)(bipym)]·dmf (1) together with the atom-labelling scheme**Figure 2.** Projections of the overlapping mode of [Pt(mnt)(bipym)] molecules (a) perpendicular and (b) parallel to the molecular plane

(av. 2.310 Å),¹⁸ *trans*-[Pt(SCN)₂(C₅H₅N)₂] [2.322(5) Å],¹⁹ and [Pt{PhNNC(S)SMe}₂] [2.284(1) Å].²⁰ The shorter Pt-S distances in the present complex seem to arise from the *trans* influence of the nitrogen atoms of the bipym ligand which acts as a π -electron acceptor. A similar Pt-S shortening owing to the presence of nitrogen *trans* to sulphur was observed in

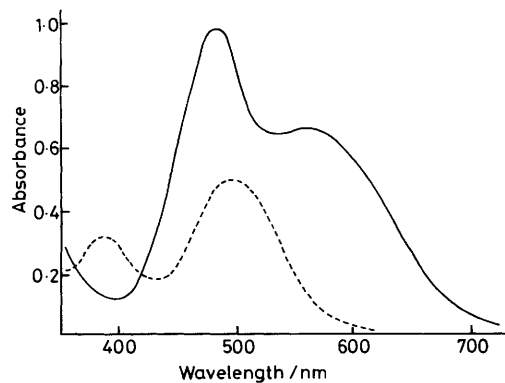


Figure 3. Electronic absorption spectra of complexes (1) (----) and (3) (—) in dimethyl sulphoxide (1.75×10^{-4} mol dm $^{-3}$)

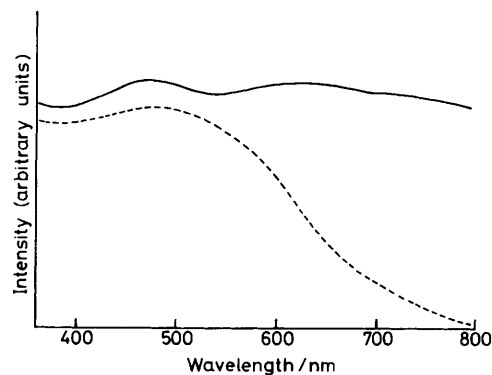


Figure 4. Powder electronic reflectance spectra of complexes (1) (----) and (3) (—)

[Pt(H₂NCH₂CH₂NH₂)(Me₂SO)₂][PF₆]₂ [Pt-S 2.248(6) Å].²¹ On the other hand, the *trans* influence of the Pt-S bonding causes lengthening of the Pt-N distances [2.033(9), 2.069(8) Å], which can be compared with that of [Pt{PhNNC(S)SMe₂}]₂ [1.966(4) Å]²⁰ having *trans* N-Pt-N bonding. A similar Pt-N lengthening is observed in [Pt(H₂NCH₂CH₂NH₂)(Me₂SO)₂][PF₆]₂ [2.062(9) and 2.067(8) Å].²¹

Figure 2 shows projections of the [Pt(mnt)(bipym)] molecules perpendicular and parallel to the molecular plane. The molecules form a one-dimensional column although it deviates greatly from a column formed by a linear metal-metal sequence, while in the crystal the solvated dmf molecule has no significant contact with the [Pt(mnt)(bipym)] moieties. Pt-Pt distances in the column are considerable (3.65 and 4.47 Å) and the shortest intermolecular sulphur-nitrogen distance (3.62 Å) seems to result from a weak electrostatic interaction between electron-donor sulphur and π -electron-acceptor pyrimidyl nitrogen atoms, the polarized state of this complex being described later. Separations between the molecular planes within the column are 3.36 and 3.53 Å, which are far longer than those of one-dimensional metallic platinum complexes (2.8–2.9 Å).²²

Electronic Absorption and Reflectance Spectra of the PtS₂N₂-type Complexes.—Figure 3 illustrates the electronic absorption spectra of complexes (1) and (3). The intense band at 478 nm observed for (3) is assigned to the dmit ligand transition,⁵ and the shoulder at 560 nm to the ligand-to-ligand charge-transfer (l.l.c.t.) transition as previously described.^{2–5} The latter displays appreciable negative solvatochromism, indicating a polarized ground state for the complex.⁵ The spectrum of (1)

Table 4. Electronic absorption band maxima (nm) of the PtS₂N₂-type complexes*

Complex	dmit or mnt ligand transition	ligand-to-ligand c.t. transition
(1) [Pt(mnt)(bipym)]-dmf	390 (2.99)	493 (3.01)
(2) [Pt(mnt)(epa)]	384 (3.04)	508 (3.22)
(3) [Pt(dmit)(bipym)]	478 (4.29)	560 (4.00)
(4) [Pt(dmit)(epa)]	482 (4.01)	580 (3.91)

* Measured in dimethyl sulphoxide. Apparent log ϵ in parentheses.

Table 5. Anodic peak potentials of the PtS₂N₂-type complexes determined by cyclic voltammetry*

Complex	E_{pa} /V vs. s.c.e.
(1)	1.32
(2)	1.30
(3)	0.80
(4)	0.76

* Measured in dmf: supporting electrolyte 0.1 mol dm $^{-3}$ [NBu₄]⁺ClO₄⁻, sweep rate 50 mV s $^{-1}$

also shows the mnt ligand transition and l.l.c.t. transition bands, which appear at somewhat shorter wavelengths than those of (3). Table 4 summarizes the electronic absorption band maxima for the PtS₂N₂-type complexes.

The powder electronic reflectance spectra of (1) and (3) are illustrated in Figure 4. The spectrum of (1) shows the bands corresponding to those observed in solution, suggesting no significant intermolecular interaction in the solid state. This is consistent with the weak, electrostatic S...N interaction displayed in the crystal structure of (1). On the other hand, the spectrum of (3) exhibits a tail-broadening band to a longer wavelength, which suggests some intermolecular interaction. Since in the solid state the [Pt(dmit)(bipym)] molecules are also likely to assume a columnar structure through S...N electrostatic interaction, similar to that of the mnt analogue, the intermolecular interaction may come from sulphur-sulphur contacts between dmit ligands, as observed for dmit-metal complexes such as [epy]₂[Cu(dmit)₂] (epy = *N*-ethylpyridinium)¹⁰ and [mpaz]₂[V(dmit)₃] (mpaz = *N*-methylphenazinium).²³

Oxidation of the PtS₂N₂-type Complexes by Iodine- and Bromine-doping.—A cyclic voltammogram of (4) measured in dmf indicated a reversible oxidation wave at $E_{\frac{1}{2}}^0 = 0.74$ V (vs. s.c.e.) (anode peak potential – cathode peak potential = 60 mV), although complexes (1)–(3) have shown irreversible oxidation waves. Table 5 summarizes anode peak potentials of complexes (1)–(4) determined from cyclic voltammetry in dmf. The oxidation potentials of (1) and (2) are *ca.* 0.5 V higher than those of the dmit analogues (3) and (4), which is consistent with the higher l.l.c.t. transition energies of the former compared with the latter.

The dmit complexes (3) and (4) have been doped with iodine by reacting the finely powdered complexes suspended in hexane with an excess amount of iodine. Complex (5) exhibits a Raman peak at 106 cm $^{-1}$ which is assignable to the symmetric stretching of the I₃⁻ ion.²⁴ Complex (6), obtained by reacting (3) with a larger excess of iodine, shows a Raman peak at 166 cm $^{-1}$, which is reasonably ascribed to the I₅⁻ ion.^{25,26} Thus, complexes (5) and (6) are formulated as [Pt(dmit)(bipym)][I₃]_{0.53} and [Pt(dmit)(epa)][I₅]_{0.54}, respectively. These findings indicate that (3) can be oxidized by a *ca.* 0.5 molar fraction of iodine. Iodine-doped complexes (7) and (8) also show Raman peaks at 106 and 166 cm $^{-1}$, respectively, from which they are formulated

Table 6. Binding energies of Pt 4f electrons of the PtS₂N₂-type complexes and their halogen-doped derivatives as determined by x.p.s.

Complex	Binding energy/eV	
	Pt 4f _{7/2}	Pt 4f _{5/2}
(1)	75.7	72.4
(2)	75.3	72.0
(3)	75.1	71.9
(4)	75.0	71.7
(5)	75.1	72.0
(6)	74.9	71.8
(7)	75.4	72.3
(8)	75.1	72.0
(9)	77.0, 75.1	74.0, 71.4
(10)	77.2, 75.2	74.0, 72.1
(11)	77.0	73.7
(12)	77.3	74.1

Table 7. Electrical conductivities (σ) and activation energies (E_a) of PtS₂N₂-type complexes and their halogen-doped derivatives*

Complex	$\sigma(25^\circ\text{C})/\text{S cm}^{-1}$	E_a/eV
(1)	$<10^{-12}$	
(2)	$<10^{-12}$	
(3)	2.5×10^{-9}	0.73
(4)	5.9×10^{-10}	0.34
(5)	1.0×10^{-7}	0.51
(6)	3.8×10^{-6}	0.27
(7)	5.9×10^{-8}	0.34
(8)	1.1×10^{-7}	0.22
(9)	$<10^{-12}$	
(10)	2.2×10^{-7}	0.25
(11)	1.1×10^{-4}	0.71
(12)	$<10^{-12}$	

* Measured for compacted pellets.

as [Pt(dmit)(epa)][I₃]_{0.63} and [Pt(dmit)(epa)][I₅]_{0.67}; i.e. complex (4) can be oxidized with a slightly higher fraction of iodine than complex (3).

On the other hand, the mnt analogues (1) and (2) could not be doped with iodine. This may be ascribed to their high oxidation potentials. Complex (2) in the solid state, however, reacted with bromine in dmf to form [PtBr₂(mnt)(epa)] (12) which contains a Pt^{IV} atom as described later. A powder of (2) was doped with excess bromine in hexane to afford the bromine-doped complex [Pt(mnt)(epa)]Br_{0.52} (9). The dmit analogues (3) and (4) were also doped with bromine to form [Pt(dmit)(bipym)]Br_{1.8} (10) and [Pt(dmit)(epa)]Br_{3.1} (11).

The iodine-doped dmit complexes (5)–(8) exhibited anisotropic broad e.s.r. signals around $g = 2.06$ which are similar to those of [Pt(dmit)(phen)]I_{1.9} (phen = 1,10-phenanthroline)⁵ and [NBu₄][Rh(dmit)₂].²⁷ Thus, partial oxidation of [Pt(dmit)L] (L = bipym or epa) with iodine occurs essentially at the dmit ligand. This is confirmed by the fact that binding energies of the Pt 4f electrons of the iodine-doped complexes, determined from x.p.s., are very close to those of the original PtS₂N₂-type complexes (see Table 6).

X.p.s. of bromine-doped complexes (9) and (10) exhibit bands due to Pt^{IV} species as well as those of Pt^{II}, while (11) and (12) show only the x.p.s. bands ascribed to Pt^{IV} species. The bromine-doped complexes are essentially diamagnetic, although (11) gives an intense e.s.r. signal similar to that of (5). Thus, in the paramagnetic complex (11), the dmit moiety also seems to be oxidized.

Table 7 summarizes electrical conductivities at 25°C and activation energies for the electrical conduction measured for

compacted pellets of the complexes. [Pt(mnt)L] (L = bipym or epa) are almost insulators. The dmit analogues behave as semiconductors in the range -20 to $+40^\circ\text{C}$, although their conductivities are very small. This may arise from intermolecular interaction through the dmit sulphur atoms. Although the mnt–Pt^{IV} complexes formed by bromine-doping of the mnt–Pt^{IV} analogues are insulators, the halogen-doped dmit complexes exhibit 10^2 – 10^6 higher conductivities than the original [Pt(dmit)L] complexes. This may be ascribed to the formation of electrical conduction pathways through sulphur–sulphur contacts of the oxidized dmit moieties.

Acknowledgements

We thank Professor K. Nakatsu, Kwansai Gakuin University, for use of the programs for the structure solution and refinement. This work was partially supported by a Matsuda Research Grant, for which we thank the Matsuda Foundation.

References

- J. S. Miller (ed.), 'Extended Linear Chain Compounds,' Plenum Press, New York, 1983, vol. 3.
- T. R. Miller and I. G. Dance, *J. Am. Chem. Soc.*, 1973, **95**, 6970.
- A. Vogler and H. Kunkely, *J. Am. Chem. Soc.*, 1981, **103**, 1559.
- L. Kumar, K. H. Puthraya, and T. S. Srivastava, *Inorg. Chim. Acta*, 1984, **86**, 173.
- G. Matsubayashi, M. Hirao, and T. Tanaka, *Inorg. Chim. Acta*, 1988, **144**, 217.
- J. Lock and J. A. McCleverty, *Inorg. Chem.*, 1966, **5**, 1157.
- K. Kawakami, T. Ohara, G. Matsubayashi, and T. Tanaka, *Bull. Chem. Soc. Jpn.*, 1975, **48**, 1440.
- K. Ueyama, G. Matsubayashi, and T. Tanaka, *Inorg. Chim. Acta*, 1984, **87**, 143.
- G. Matsubayashi, K. Kondo, and T. Tanaka, *Inorg. Chim. Acta*, 1983, **69**, 167.
- G. Matsubayashi, K. Takahashi, and T. Tanaka, *J. Chem. Soc., Dalton Trans.*, 1988, 967.
- S. Araki, K. Ishida, and T. Tanaka, *Bull. Chem. Soc. Jpn.*, 1978, **51**, 407.
- 'International Tables for X-Ray Crystallography,' Kynoch Press, Birmingham, 1974, vol. 4.
- C. K. Johnson, ORTEP-II, Report ORNL 5138, Oak Ridge National Laboratory, Oak Ridge, Tennessee, 1976.
- A. Kobayashi, Y. Sasaki, H. Kobayashi, A. E. Underhill, and M. M. Ahmad, *J. Chem. Soc., Chem. Commun.*, 1982, 390.
- M. M. Ahmad, D. J. Turner, A. E. Underhill, A. Kobayashi, Y. Sasaki, and H. Kobayashi, *J. Chem. Soc., Dalton Trans.*, 1984, 1759.
- A. Kobayashi, Y. Sasaki, H. Kobayashi, A. E. Underhill, and M. M. Ahmad, *Chem. Lett.*, 1984, 305.
- A. Kobayashi, T. Mori, Y. Sasaki, H. Kobayashi, M. M. Ahmad, and A. E. Underhill, *Bull. Chem. Soc. Jpn.*, 1984, **57**, 3262.
- J. P. Fackler, jun., *J. Am. Chem. Soc.*, 1972, **94**, 1009.
- M. R. Caira and L. R. Nassimbeni, *Acta Crystallogr., Sect. B*, 1974, **31**, 581.
- G. Dessy and V. Fares, *Acta Crystallogr., Sect. B*, 1980, **36**, 2266.
- G. Bruno, G. Bombieri, G. Alibrandi, S. Lanza, and R. Romeo, *Crystr. Struct. Commun.*, 1982, **11**, 1369.
- J. S. Miller and A. J. Epstein, *Prog. Inorg. Chem.*, 1976, **21**, 40.
- G. Matsubayashi, K. Akiba, and T. Tanaka, unpublished work.
- B. N. Diel, T. Inabe, J. W. Lyding, K. F. Schoch, jun., C. R. Kannewurf, and T. J. Marks, *J. Am. Chem. Soc.*, 1983, **105**, 1551.
- M. A. Cowie, A. Cleizes, G. W. Grynckewich, D. W. Kalina, M. S. McClure, R. P. Scaaringe, R. C. Teitelbaum, S. L. Ruby, J. A. Ibers, C. R. Kannewurf, and T. J. Marks, *J. Am. Chem. Soc.*, 1979, **101**, 2921.
- R. C. Teitelbaum, S. L. Ruby, and T. J. Marks, *J. Am. Chem. Soc.*, 1980, **102**, 3322.
- K. Yokoyama, G. Matsubayashi, and T. Tanaka, *Polyhedron*, 1988, **7**, 379.